The Electron Transfer Complexes of Cytochrome *c* Peroxidase from *Paracoccus denitrificans*[†]

Graham W. Pettigrew,*[,‡] Celia F. Goodhew,[‡] Alan Cooper,[§] Margaret Nutley,[§] Kornelia Jumel,[||] and Stephen E. Harding[||]

Department of Preclinical Veterinary Sciences, Royal (Dick) School of Veterinary Studies, University of Edinburgh, Summerhall, Edinburgh EH9 1QH, U.K., Department of Chemistry, University of Glasgow, Glasgow G12 8QQ, U.K., and Centre for Macromolecular Hydrodynamics, University of Nottingham, Sutton Bonington, Nottingham LE12 5 RD, U.K.

Received November 7, 2002; Revised Manuscript Received December 20, 2002

ABSTRACT: We have used microcalorimetry and analytical ultracentrifugation to test the model proposed in Pettigrew et al. [(1999) *J. Biol. Chem. 274,* 11383−11389] for the binding of small cytochromes to the cytochrome *c* peroxidase of *Paracoccus denitrificans*. Both methods reveal complexity in behavior due to the presence of a monomer/dimer equilibrium in the peroxidase. In the presence of either Ca^{2+}, or higher ionic strength, this equilibrium is shifted to the dimer. Experiments to study complex formation with redox partners were performed in the presence of Ca^{2+} in order to simplify the equilibria that had to be considered. The results of isothermal titration calorimetry reveal that the enzyme can bind two molecules of horse cytochrome *c* with K_d values of 0.8 μM and 2.5 μM (at 25 °C, pH 6.0, $I = 0.026$) but only one molecule of *Paracoccus* cytochrome *c*-550 with a K_d of 2.8 μM, molar binding ratios confirmed by ultracentrifugation. For both horse cytochrome *c* and *Paracoccus* cytochrome *c*-550, the binding is endothermic and driven by a large entropy change, a pattern consistent with the expulsion of water molecules from the interface. For horse cytochrome *c*, the binding is weakened 3-fold at $I = 0.046$ M due to a smaller entropy change, and this is associated with an increase in enzyme turnover. In contrast, neither the binding of cytochrome *c*-550 nor its oxidation rate is affected by raising the ionic strength in this range. We propose that, at low ionic strength, horse cytochrome *c* is trapped in a nonproductive orientation on a broad capture surface of the peroxidase.

Biological electron transfer remains a poorly understood phenomenon. The requirement for specificity leads to the burial of potentially promiscuous redox centers within proteins. However, this compromises the speed of electron transfer since only small areas of the protein surface may be redox active or represent entry points into rapid conduction routes to the buried redox center [but not all agree that conduction pathways are a valid concept (*2*)]. It has been proposed that electrostatic preorientation prior to collision and lateral fluidity in the encounter complex are factors which allow enhanced electron transfer rates (*3*−*6*).

Lateral fluidity implies that there exists a range of relative orientations of the two proteins that are interlinked through a landscape of low-energy barriers. A striking illustration of this is the analysis by Liang and co-workers (*7*) of the binding of cytochrome b_5 to myoglobin. Binding is described by a family of conformations in dynamic exchange, only a small proportion of which are active in electron transfer. A feature of redox proteins is that there is often very little conformational difference between the reduced and oxidized forms. Thus not only must lateral diffusion on the surface be an energetically accessible process but the association with the surface must be relatively weak to allow prompt dissociation once the electron transfer has occurred.

This relative instability of biological electron transfer complexes limits, to some extent, the approaches that can be used to study them. The clearest indication of this is the relatively few electron transfer complexes that have been cocrystallized, the best example being the yeast cytochrome *c* peroxidase/cytochrome *c* complex (*8*). Many studies have implicated a single high-affinity site located in the region of Ala 193 and Ala 194 and leading to an electron transfer pathway to Trp 191 which is in van der Waals contact with the heme group (reviewed in ref *9*). This high-affinity site can be occupied by either horse cytochrome *c* or the orthologous yeast cytochrome *c* but with strikingly different thermodynamic parameters (see Discussion). However, there has been a long-standing debate about the presence or otherwise of a second site of low affinity (reviewed in ref *9*). Such a site was suggested by the dynamic docking studies of Northrup et al. (*4*) and has been detected by both kinetic and thermodynamic analysis. Particularly relevant to this study is the investigation of Leesch et al. (*9*), who used isothermal calorimetry to demonstrate the presence of the low-affinity second site. They then manipulated the affinity of the putative site by a K149E mutation and found a 3-fold

[†] G.W.P. acknowledges the support of BBSRC (project grant 15B/13005). The microcalorimetry facility (Glasgow) and the analytical ultracentrifugation facility (Nottingham) are funded jointly by the BBSRC and EPSRC.

* To whom correspondence should be addressed. Telephone: 0131 650 6135. Fax: 0131 650 6576. E-mail: g.pettigrew@ed.ac.uk.

[‡] University of Edinburgh.

[§] University of Glasgow.

[||] University of Nottingham.

10.1021/bi027125w CCC: $25.00
Published on Web 01/24/2003

increase in the binding affinity, consistent with the more negative surface on the peroxidase for binding the positively charged cytochromes.

We have studied the cytochrome *c* peroxidase of *Paracoccus denitrificans* and its redox partners as a model system in which to investigate some of these aspects. At the end of one catalytic turnover, the oxidized peroxidase requires two electrons to restore it to its active form in which one of the two heme groups (called the electron transferring or E heme) is Fe^{2+} and the other (called the peroxidatic or P heme) is Fe^{3+}. In previous studies (*1*), using molecular docking simulation, we have shown that the physiological redox partner, *Paracoccus* cytochrome *c*-550, preferentially binds close to the E heme with only 16 Å between heme irons. On the other hand, horse cytochrome *c*, which is as competent kinetically as the physiological redox partner, prefers to bind at a position between the two heme groups.

Complex formation was also studied by the perturbation in ^{1}H NMR spectra of the heme methyl resonances of both the peroxidase and the donor cytochromes (*1*). These results were again consistent with distinct binding sites for the horse cytochrome *c* and the *Paracoccus* cytochrome *c*-550. The existence of two binding sites raises the possibility that the two electrons required to restore the active form of the enzyme after a turnover are delivered synchronously rather than sequentially.

In this paper we use microcalorimetry and analytical ultracentrifugation as independent tests of these binding studies and the hypotheses that derive from them. In both methods, the aggregation state of the peroxidase itself is a factor in the interpretation of the results. Previous studies (*10*−*13*) had suggested that various factors (including reduction to the mixed valence enzyme, higher ionic strength, and the presence of Ca^{2+}) shifted a monomer/dimer equilibrium of the peroxidase toward the dimer and that the dimer was the active species. However, there is very little direct evidence for this equilibrium. We have therefore investigated conditions where the peroxidase is shifted completely to a dimeric state, and we have used that simplifying condition to study the binding of donor cytochromes. Our results therefore contribute not only to an understanding of the protein/protein association required for electron transfer but also to an understanding of the monomer/dimer equilibrium of the peroxidase itself.

MATERIALS AND METHODS

Source of Proteins. Cytochrome *c* peroxidase and cytochrome *c*-550 were purified from *P. denitrificans* (ATCC 19367, NCIB 8944, LMD 52.44) [also called *Paracoccus pantotrophus* (*14*)] as described by Goodhew et al. (*15*) and used in the oxidized state. Horse cytochrome *c* (type VI) was obtained from Sigma and used in the oxidized state. Enzyme and cytochrome concentrations were determined using extinction coefficients of 250 mM^{-1} cm^{-1} (cytochrome *c* peroxidase, 409 nm), 108 mM^{-1} cm^{-1} (cytochrome *c*-550, 410 nm), and 109 mM^{-1} cm^{-1} (horse cytochrome *c*, 408 nm).

Analytical Ultracentrifugation. Partial specific volumes of the proteins were calculated from the amino acid compositions and are 0.7318 mL/g (cytochrome *c* peroxidase), 0.735 mL/g (cytochrome *c*-550), and 0.744 mL/g (horse cytochrome *c*). Protein solutions were equilibrated with the appropriate buffer by molecular exclusion chromatography on Sephadex G-25 and were used at a concentration ranging from 2 to 40 μM. The Beckman Optima XL-A or XL-I (Beckman, Palo Alto, CA) analytical ultracentrifuges, equipped with scanning absorption optics, were used in all investigations. The sedimentation velocity experiments were carried out at 45000 rpm, 25 °C, and the sedimentation equilibrium experiments at 17000 rpm, 25 °C. Sedimentation coefficients (s)[1] and sedimentation equilibrium profiles were obtained by scanning at 410, 440, or 530 nm depending on the protein concentration in the cell. The extinction coefficients of the cytochrome *c* peroxidase at these wavelengths are 250, 33, and 20 mM^{-1} cm^{-1}, respectively. The DCDT+ program of Philo (*16*) was used to analyze groups of boundaries to derive sedimentation coefficients. This method is based on the time-derivative method developed by Stafford (*17*, *18*) which fits Gaussian functions to the so-called $g(s^*)$ distribution: for a given component, the breadth of this distribution also facilitates an estimate for the translational diffusion coefficient D^*. The "*" in s^* and D^* indicates the inability to distinguish whether intensity on either side of a peak really represents material sedimenting with that s value or is merely broadening due to diffusion of material sedimenting at the s value of the peak. Sedimentation and diffusion coefficients were corrected to standard solvent conditions (the viscosity and, for the sedimentation coefficient, the density of water at 20 °C) using the SEDNTERP program (based on ref *19*). The derivation of a value of M_r from the sedimentation velocity experiments is based on the s/D ratio and is dependent on reliable estimates of both. In the case of interacting systems such as those described here, a boundary may contain more than one species in equilibrium, and M_r values derived from such a boundary can only be regarded as rough estimates. In such a case, the diffusion coefficient is likely to be an overestimate and the M_r an underestimate. Sedimentation equilibrium experiments were run until two scans taken at 4 h intervals could be perfectly overlaid, indicating that equilibrium had been achieved. Sedimentation equilibrium data were analyzed in terms of an association constant reported in reciprocal absorbance units, using Origin 4.1 software from Beckman Instruments (Palo Alto, CA). Molar dissociation constants were calculated by adjusting for path length (1.2 cm) and using the appropriate extinction coefficient. Nonideality effects were assumed to be negligible at the dilute concentrations studied.

Microcalorimetry. Protein solutions were equilibrated with the appropriate buffer by molecular exclusion chromatography on Sephadex G-25. The titrant solution was then concentrated by centrifugation above a Vivaspin membrane (M_r cutoff 5000). Protein concentrations were determined using the extinction coefficients noted above.

For isothermal titration calorimetry, the protein solutions were degassed and the target cytochrome *c* peroxidase was

[1] Abbreviations: EGTA, ethylene glycol bis(β-aminoethyl ether)-*N*,*N*,*N*′,*N*′-tetraacetic acid; Mes, 2-(*N*-morpholino)ethanesulfonic acid; Hepes, *N*-(2-hydroxyethyl)piperazine-*N*′-2-ethanesulfonic acid; DSC, differential scanning calorimetry; ITC, isothermal titration calorimetry; D, diffusion coefficient; s, sedimentation coefficient; $\Delta H°$, standard enthalpy change; ΔH_v, van't Hoff standard enthalpy change; ΔH_c, calorimetric standard enthalpy change; $\Delta G°$, standard free energy change; $\Delta S°$, standard entropy change.

placed in the sample chamber of the VP-ITC microcalorimeter (Microcal). The syringe was filled with a solution of the probe protein, and successive injections of 10 μL were delivered into the stirred chamber (310 rpm). The duration of the additions was 20 s, and they were 180 s apart. The instrument records the heat evolved or absorbed in the sample chamber by adjusting a heating circuit to maintain a constant temperature, and the data are analyzed within Microcal origin software which fits on the basis of iteration within a Marquandt routine. Data were fitted using models for one set of sites and for two independent sets of sites. The value of K_d was used to calculate the standard Gibbs free energy change ($\Delta G°$). It is conventional to assume (with little error) that the experimentally determined ΔH is identical to the standard enthalpy change ($\Delta H°$). The standard free energy change and standard enthalpy change were used to calculate a standard entropy change ($\Delta S°$).

The possibility that the observed $\Delta H°$ values are a combination of the enthalpy change associated with the protein/protein interaction and an enthalpy change in the buffer due to protons released or taken up in the formation of the complex was investigated by carrying out experiments in two buffers of differing enthalpy of ionization and solving the equation

$$\Delta H_{obsd} = \Delta H_{binding} + n\Delta H_{buffer\ protonation}$$

The enthalpies of ionization of the Mes and cacodylate buffers were +16.72 and −2.34 kJ mol^{-1}, respectively (*23*). (*Note*: cacodylate is toxic by inhalation of the dust or ingestion. Care is required in handling.)

For differential scanning calorimetry (DSC), a degassed protein solution was placed in the sample chamber of the VP-DSC (Microcal) and the temperature raised from 15 to 100 °C at a scan rate of 60 °C h^{-1}. The thermogram is analyzed using Microcal Origin software using a standard non-two-state model which yields independent estimates of the calorimetric (ΔH_c) and van't Hoff (ΔH_v) enthalpies.

Molecular Docking Simulation. Docking was performed as described in ref *1* using the algorithm BiGGER developed by Palma et al. (*20*). This algorithm performs a complete and sytematic search of the rotational space of one protein relative to the other, generating a large number of candidate docking geometries based solely on the complementarity of the molecular surfaces. This initial prefilter of solutions is required to make the computation of a more complete set of energies of interaction manageable. The 1000 best solutions thus generated were finally evaluated and ranked according to a combination of additional interaction criteria that include electrostatic energy of interaction, relative solvation energy, and the relative propensity of adjacent side chains to interact.

A cytochrome *c* peroxidase monomer with a horse cytochrome *c* already bound at the "between-hemes" site (the highest ranking solution of ref *1*) was used as the target for the binding of a second horse cytochrome *c* molecule. The target and the probe proteins were each broken down into a grid of 1.2 Å cubes, and 15° rotations of the probe against the target were performed along with systematic translations to generate the candidate group of 1000 solutions.

RESULTS

The Monomer/Dimer Equilibrium of the Peroxidase. (i) Analytical Ultracentrifugation. The sedimentation velocity profiles of cytochrome *c* peroxidase centrifuged at pH 7.5 in the presence of Ca^{2+}, in the presence of EGTA, and with no addition were analyzed by the DCDT+ method (*16*), and the distribution of sedimentation coefficients is shown in Figure 1. It is clear that marked changes in aggregation of the protein are occurring. In the presence of Ca^{2+}, an $s_{20,w}$ value of 4.78 S was obtained, which, together with the estimate of *D*, yielded M_r 73000, a value proposed to reflect the dimer (theoretical value based on sequence, 75026). With no addition of Ca^{2+}, the monomer/dimer equlibrium is shifted toward the monomeric form and an $s_{20,w}$ value of 2.69 S. In the presence of EGTA, the protein shifts further to the monomer and an $s_{20,w}$ value of 2.54 S. This value, together with the estimate of *D*, yields M_r 32000, a value proposed to reflect the monomer (theoretical value based on sequence, 37513).

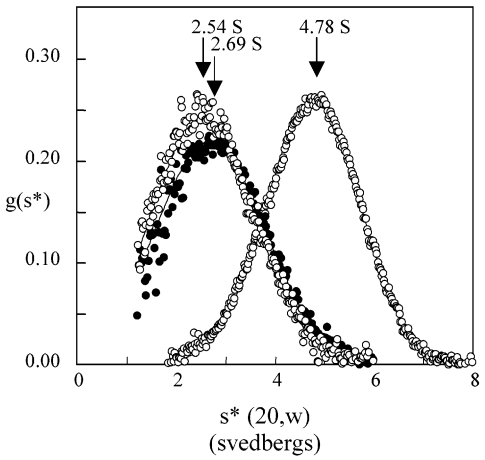

FIGURE 1: Sedimentation velocity profiles for the monomeric and dimeric states of cytochrome *c* peroxidase. Paired scans within a set of 10 sequential scans were used to produce a distribution of sedimentation coefficients using the DCDT+ method of Philo (*16*) and Stafford (*17*, *18*). Centrifugation was of 10 μM cytochrome *c* peroxidase in 10 mM Hepes, pH 7.5, containing (a) no further addition (closed circles, 2.69 S), (b) 1 mM EGTA (open circles, 2.54 S), and (c) 5 mM $CaCl_2$ (open circles, 4.78 S). The vertical axis is in absorbance units/Svedberg.

In addition to Ca^{2+}, elevated ionic strength and the reduction of the high-potential heme group also shift the enzyme toward the dimeric state (results not shown). For example, the $s_{20,w}$ value obtained under the conditions of Figure 1a but with the addition of 50 mM NaCl was 4.67 S, very close to the value in the presence of 5 mM Ca^{2+}(4.78 S).

Sedimentation equilibrium experiments were conducted at pH 6.0, a pH at which previous studies have proposed a greater proportion of dimer than at pH 7.5. When the final protein distribution at equilibrium was analyzed as a single homogeneous species, satisfactory fits were obtained for the M_r values shown in Table 1. In the absence of Ca^{2+}, these apparent M_r values rose with rising protein concentration, consistent with a monomer/dimer equilibrium. The data also satisfactorily fitted a monomer/dimer equilibrium in which the monomer was set at 37500. Using this form of analysis, in the absence of Ca^{2+}, a value of 12 μM was obtained for the K_d.

In the presence of Ca^{2+}, M_r values of 68700−72500 were obtained. Extrapolation to zero protein concentration gave an M_r close to the expected value for a dimer (75026).

Table 1: Sedimentation Equilibrium Analysis of *Paracoccus* Cytochrome *c* Peroxidase[a]

protein concn (μM)	Ca^{2+}	apparent M_r[b]	K_d[c] (μM)
2	−	48000	
10	−	54000	12
40	−	59100	
2	+	72500	
10	+	69100	
40	+	68700	

[a] Sedimentation equilibrium was carried out in 10 mM Mes and 10 mM NaCl, pH 6.0, in the absence or presence of 2 mM Ca^{2+}. [b] Analyzed as a single homogeneous species. [c] Analyzed as a monomer/dimer equilibrium with the monomer set at 37500.

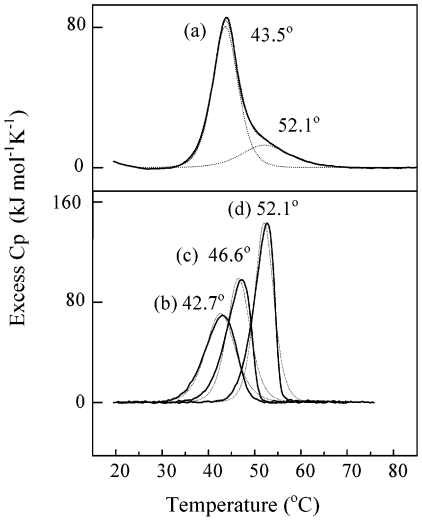

FIGURE 2: Differential scanning calorimetry of *Paracoccus* cytochrome *c* peroxidase. *Paracoccus* cytochrome *c* peroxidase (15 μM) equilibrated with the appropriate buffer was placed in the sample chamber of the instrument at 15 °C and the sample solution warmed to 100 °C. Buffer controls were subtracted from the experimental data. Conditions: (a) 10 mM Mes, 10 mM NaCl, pH 6.0; (b) 10 mM Hepes, pH 7.5; (c) 10 mM Hepes, 50 mM NaCl, pH 7.5; (d) 10 mM Hepes, pH 7.5, 2 mM $CaCl_2$. The broken lines indicate the curve fitting of two components in (a) and a single component in (b)−(d) using a standard non-two-state model.

(ii) Differential Scanning Calorimetry. The cytochrome *c* peroxidase showed a complex thermal unfolding at pH 6.0 in the absence of Ca^{2+}which was fitted by two endothermic components with transition temperatures of 43.5 °C (ΔH_c = 589 kJ mol^{-1}, ΔH_v = 460 kJ mol^{-1}) and 52.1 °C (ΔH_c = 175 kJ mol^{-1}, ΔH_v = 259 kJ mol^{-1}) (Figure 2a). At pH 7.5 in the absence of Ca^{2+}, a single transition of 42.7 °C (ΔH_c = 602 kJ mol^{-1}, ΔH_v = 390 kJ mol^{-1}) was sufficient to fit the data (Figure 2b), and this shifted to 46.6 °C in the presence of 50 mM NaCl (ΔH_c = 652 kJ mol^{-1}, ΔH_v = 514 kJ mol^{-1}) (Figure 2c) and 52.1 °C (ΔH_c = 777 kJ mol^{-1}, ΔH_v = 644 kJ mol^{-1}) in the presence of 2 mM Ca^{2+} (Figure 2d). In each case, the ΔH_v is somewhat smaller than ΔH_c, probably reflecting a broader transition and a breakdown of the simple two-state model assumption due to a significantly populated intermediate in the unfolding process.

(iii) Isothermal Titration Calorimetry. The titration of cytochrome *c* peroxidase with horse cytochrome *c* was studied at both pH 6.0 and pH 7.5, the two pH values used in previous kinetic and spectroscopic analyses and also used above in the ultracentrifugation and DSC experiments. At both pH values, but especially pronounced at pH 7.5 (Figure 3a), the titration results showed complexity (in the form of an initially rising heat change as the titration progressed) which probably indicates a ligand-induced change in oligomerization leading to a cooperative binding effect. The presence of Ca^{2+} simplified the titration (Figure 3b) (see next section).

Binding of Paracoccus Cytochrome c Peroxidase to Horse Cytochrome c and Paracoccus Cytochrome c-550. (i) Isothermal Titration Calorimetry. The endothermic association of cytochrome *c* peroxidase and horse cytochrome *c* in the presence of Ca^{2+} is shown in Figure 3b for pH 7.5, and the thermodynamic parameters for titrations at both pH 6.0 and pH 7.5 are shown in Table 2. For the results of Figure 3b at pH 7.5, a simple fitting of a single-set-of-sites yields an *N* value of 1.64. However, the data can also be fitted at least as well by a two-sets-of-sites model which yields two separate K_d values (Table 2). A similar pattern is observed at pH 6.0 (Table 2). The titration of cytochrome *c* peroxidase with *Paracoccus* cytochrome *c*-550 fitted a single-set-of-sites model with a molar binding ratio of 1.04 (Figure 3c, Table 2).

The observed heat changes for both proteins were buffer dependent, indicating that binding was accompanied by loss of a fractional proton from the proteins and its uptake by the buffer (Table 2). There is 0.3 proton released on binding the *Paracoccus* cytochrome *c*-550 to the cytochrome *c* peroxidase and 0.46 proton released for the corresponding binding of horse cytochrome *c* at this pH. The thermodynamic parameters corrected for this proton release are included in Table 2.

An increase in ionic strength from 0.026 to 0.046 M weakens the binding of horse cytochrome *c* by a factor of 3 on the basis of the one-set-of-sites K_d value (Table 2). This is associated with a diminished entropic driving force, although the enthalpy change actually becomes somewhat less unfavorable. In the case of the cytochrome *c*-550, the increase in ionic strength has little effect on K_d, and what effect there is, is again entropic in origin.

(ii) Sedimentation Velocity Ultracentrifugation. In the presence of horse cytochrome *c* or cytochrome *c*-550, the sedimentation coefficient of the boundary containing cytochrome *c* peroxidase increased, indicating binding (Figure 4). Analysis of the absorbances associated with the leading boundary and any trailing boundary allowed the calculation of the bound cytochrome in relation to the added total cytochrome (Figure 5). The fitted solid lines of Figure 5 show that these results are consistent with a molar binding ratio of 2:1 for horse cytochrome *c* and 1:1 for cytochrome *c*-550. The leading boundary at 4:1 horse cytochrome *c* had a sedimentation coefficient of 6.18 S (Figure 6a) which, together with an estimate of *D*, yields M_r 108000. The leading boundary at 4:1 cytochrome *c*-550 had a sedimentation coefficient of 5.55 S (Figure 6b) which, together with an estimate of *D*, yields M_r 94000. The sedimentation coefficient of the cytochrome *c* peroxidase alone, together with an estimate of *D*, yields an M_r value close to that of the dimer of 75026. The trailing boundaries are the free cytochrome *c* in each case.

Molecular Docking of Two Molecules of Horse Cytochrome c to the Surface of the Paracoccus Cytochrome c Peroxidase. Using the highest ranking docking solution (*1*)

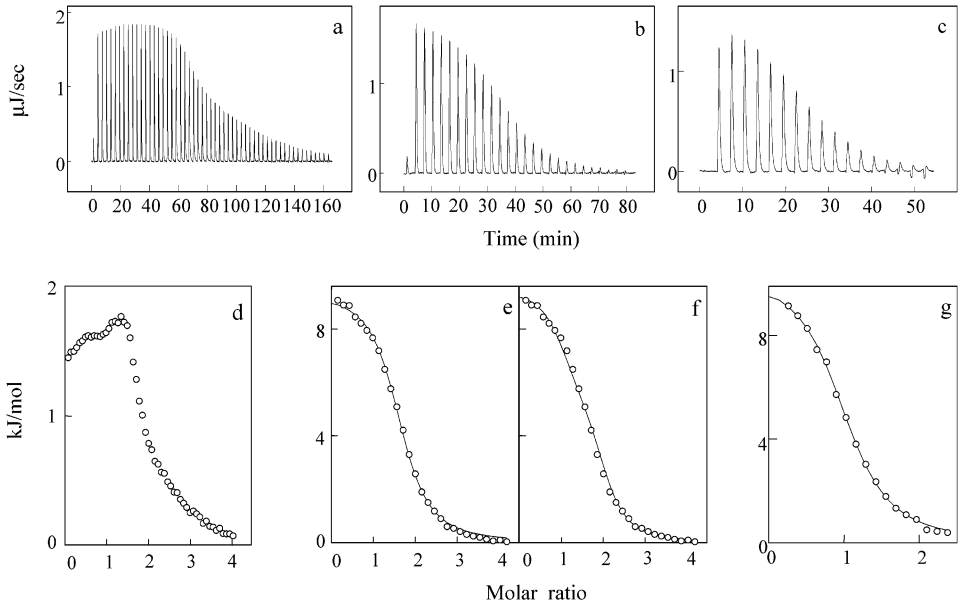

FIGURE 3: Isothermal titration calorimetry of the binding of horse cytochrome *c* and *Paracoccus* cytochrome *c*-550 to *Paracoccus* cytochrome *c* peroxidase. Horse cytochrome *c*, *Paracoccus* cytochrome *c*-550, and *Paracoccus* cytochrome *c* peroxidase were equilibrated in the appropriate buffer by passage down a Sephadex G-25 molecular exclusion column. The microcalorimetry chamber contained degassed cytochrome *c* peroxidase at a known concentration between 25 and 30 μM. The syringe contained degassed horse ferricytochrome *c* or *Paracoccus* ferricytochrome *c*-550 in the same buffer at a known concentration between 450 and 700 μM. Each delivery of titrant was set to take 20 s with 180 s between additions. Conditions: (a) 10 mM Hepes, pH 7.5, 25 °C, horse cytochrome *c* as titrant; (b) 10 mM Hepes, pH 7.5, 2 mM $CaCl_2$, 25 °C, horse cytochrome *c* as titrant; (c) 10 mM cacodylate, pH 6.0, 10 mM NaCl, 2 mM $CaCl_2$, 25 °C, *Paracoccus* cytochrome *c*-550 as titrant. (d) Heat changes for results obtained in (a), unfitted. (e) Best fit of results obtained in (b) using a single set-of-sites site model. (f) Best fit of results obtained in (b) using a two independent sets-of-sites model. (g) Best fit of results in (c) for a single set-of-sites model.

of horse cytochrome *c* to the *Paracoccus* peroxidase as a target (in which the horse cytochrome *c* is bound in a between-hemes position), the docking of a second molecule of horse cytochrome *c* was carried out in view of the molar binding ratio of 2:1 observed in both microcalorimetry and ultracentrifugation experiments. The top-ranked result for this ternary complex is shown in Figure 7. The second horse cytochrome *c* binds at the E heme and has a ranking score of −68 compared to the value of −72 for the binary complex that was used as a target (the ranking scale is a composite of different energies of interaction, and more negative is more favorable). The top 20 solutions of this ternary dock had ranking scores between −55 and −68 and contained 12 solutions clustered at the E heme in the position of the top-ranking dock shown in Figure 7.

In contrast, in the original docking of the single horse cytochrome *c* to the cytochrome *c* peroxidase, the highest ranking solution at the E heme position was ranked 12th with a ranking score of −62.

DISCUSSION

Monomer/Dimer Equilibrium and Role of Ca^{2+}. We had previously shown that Ca^{2+} binding to a vacant site on the oxidized cytochrome *c* peroxidase (called site II) is required for the spin state transition to the active mixed valence form to take place (*12*). Investigation of the kinetics of oxidation of donor cytochromes indicated that dilute solutions of the enzyme had low activity, and this was interpreted as due to a shift toward an inactive monomer from an active dimer (*13*). It was proposed that Ca^{2+} bound to the interface of the dimer and promoted dimerization (*10*, *11*). A shift in the elution position of the enzyme on molecular exclusion chromatography in the presence of Ca^{2+} was consistent with the stabilization of the dimer by Ca^{2+} (unpublished results), but because of the nonspherical nature of both monomer and dimer, these results could not be used to derive molecular weights. As judged by spectroscopic and kinetic criteria, the formation of dimer was also promoted by lower pH and higher ionic strength (*10*−*12*).

Thus we had proposed that the activity and the binding of Ca^{2+} go hand-in-hand and are associated with the dimeric state. However, much of the evidence for this (outlined above) is indirect. Consequently, we have used differential scanning calorimetry and, in particular, ultracentrifugation to study the factors influencing the monomer/dimer equilibrium of the cytochrome *c* peroxidase.

The results presented here all confirm the strong influence of Ca^{2+} on the aggregation state of the cytochrome *c* peroxidase. Ultracentrifugation gives a direct insight into the monomer/dimer equilibrium. The sedimentation velocity experiment, conducted at pH 7.5, was consistent with a monomeric species in the presence of EGTA and a dimer in the presence of Ca^{2+}. With neither added, the enzyme at 10 μM is mostly monomeric at pH 7.5, a result consistent with previous work (*10*) which showed neither activity nor high-spin formation in the mixed valence state at this pH until Ca^{2+} was added. In the presence of EGTA, the $s_{20,w}$ value of 2.54 S, together with an estimate of *D*, yields M_r 32000, a value not particularly close to the figure of 37513 based on the known sequence. This is not too surprising as the diffusion coefficient is obtained from the boundary broadening of the velocity scans, a broadening which can be influenced by factors other than diffusion. However, the sedimentation equilibrium results are conclusive with regard

Table 2: Thermodynamic Parameters of the Binding of Cytochromes to Cytochrome *c* Peroxidase[a]

(a) Binding of Cytochromes to *Paracoccus* Cytochrome *c* Peroxidase

	buffer	pH	T (°C)	I (M)	analysis	N	K_a ($\times 10^{-5}$) (M^{-1})	K_d (μM)	$\Delta H°$ (kJ mol^{-1})	$\Delta S°$ (J K^{-1} mol^{-1})	$-T\Delta S°$ (kJ mol^{-1})
horse cyt *c*	Mes	6.0	25	0.026	one site	1.34 ± 0.02	1.3 ± 0.09	7.5	12.4 ± 0.2	140	−41.6
					two sites	(1)	12.5 ± 5.6	0.8	14.2 ± 2.8	164	−48.9
						(1)	4.0 ± 1.3	2.5	−1.5 ± 2.8	102	−30.4
	cacodylate	6.0	25	0.026	one site	1.59 ± 0.01	1.9 ± 0.06	5.4	21.2 ± 0.2	172	−51.3
					two sites	(1)	11.4 ± 0.24	0.9	19.8 ± 0.7	182	−54.2
						(1)	1.7 ± 0.14	5.9	10.4 ± 0.8	135	−40.2
	cacodylate	6.0	25	0.046	one site	1.33 ± 0.04	0.64 ± 0.04	15.7	19.5 ± 0.7	157	−46.8
					two sites	(1)	0.86 ± 0.29	11.6	25.9 ± 9.9	181	−53.9
						(1)	0.39 ± 0.08	25.9	−0.8 ± 10.3	85	−25.3
	Hepes	7.5	25	0.016	one site	1.64 ± 0.01	4.5 ± 0.3	2.2	9.4 ± 0.07	140	−41.7
					two sites	(1)	52 ± 21	0.19	9.6 ± 0.3	161	−48.0
						(1)	4.4 ± 0.6	2.3	5.4 ± 0.32	126	−37.6
cyt *c*-550	Mes	6.0	25	0.026	one site	0.9 ± 0.03	3.5 ± 0.8	2.8	4.6 ± 0.22	121	−36.1
	cacodylate	6.0	25	0.026	one site	1.04 ± 0.01	2.7 ± 0.16	3.7	10.4 ± 0.17	139	−41.4
	cacodylate	6.0	25	0.046	one site	1.09 ± 0.03	2.3 ± 0.3	4.3	9.6 ± 0.35	135	−40.2

(b) Thermodynamic Parameters Corrected for Buffer Protonation Enthalpies

	pH	T (°C)	I (M)	N	K_d (μM)	$\Delta G°$ (kJ mol^{-1})	$\Delta H°$ (kJ mol^{-1})	$\Delta S°$ (J K^{-1} mol^{-1})	$-T\Delta S°$ (kJ mol^{-1})	H^+ release
horse cyt *c*	6.0	25	0.026	one site	6.5	−29.6	20.0	166	−49.6	0.46
cyt *c*-550	6.0	25	0.026	one site	3.3	−31.3	9.6	137	−40.9	0.30

(c) Binding of Cytochromes to Yeast Cytochrome *c* Peroxidase (from Refs *22* and *23*)

	buffer	pH	T (°C)	I (M)	N	K_d (μM)	$\Delta G°$ (kJ mol^{-1})	$\Delta H°$ (kJ mol^{-1})	$\Delta S°$ (J K^{-1} mol^{-1})	$-T\Delta S°$ (kJ mol^{-1})
horse *c*	P_i	6.0	26	0.02	(1)	0.67	−35.3	8.6 ± 0.21	147	−43.9
				0.05	(1)	8.3	−29.0	9.7 ± 0.96	130	−38.7
yeast iso-1 cyt *c*	DPG	6.0	25	0.014	0.89 ± 0.05	0.06	−41.4	−27.6 ± 2.9	46	−13.8
				0.044	1.02 ± 0.02	0.15	−38.9	−19.6 ± 0.4	65	−19.3

[a] The binding of horse cytochrome *c* or *Paracoccus* cytochrome *c*-550 to *Paracoccus* cytochrome *c* peroxidase was studied in 10 mM Mes, 10 mM NaCl, and 2 mM $CaCl_2$, pH 6 ($I = 0.026$), 10 mM Hepes and 2 mM $CaCl_2$, pH 7.5 ($I = 0.016$), 10 mM cacodylate, 10 mM NaCl, and 2 mM $CaCl_2$, pH 6 ($I = 0.026$), or 10 mM cacodylate, 30 mM NaCl, and 2 mM $CaCl_2$, pH 6 ($I = 0.046$). The binding of horse cytochrome *c* to yeast cytochrome *c* peroxidase (*23*) was studied in 10 mM potassium phosphate, pH 6.0, with KNO_3 added to give $I = 0.02$. The binding of yeast iso-1 cytochrome *c* to yeast cytochrome *c* peroxidase (*24*) was studied in 10 mM dimethylglutaric acid buffer, pH 6.0, with NaCl added to bring to the ionic strength required. In the two-sets-of-independent-sites analysis the curve fitting was done using the association constant and enthalpy change as variables, and the goodness of fit was indicated by the standard deviations. The molar binding ratio is set at one per site. In the one-set-of-sites analysis, N is a variable in the fitting procedure.

to molecular weight and show a dimeric enzyme in the presence of Ca^{2+} and a protein concentration-dependent monomer/dimer equilibrium in its absence. This experiment was done at pH 6 rather than pH 7.5 and, in contrast to the results of Figure 1, shows substantial presence of dimer in the absence of added Ca^{2+} (Table 1). Again, this is consistent with previous kinetic and spectroscopic work (*10*). The same work had also found that 50 mM NaCl promoted the formation of the high-spin state in the absence of added Ca^{2+}, and again this was proposed to reflect a dimerization. In this study, the sedimentation coefficient in the presence of 50 mM NaCl (4.67 S) was very close to that obtained in the presence of 2 mM Ca^{2+} (4.78 S), confirming the promotion of dimerization by the higher ionic strength.

Isothermal titration calorimetry of the binding of horse cytochrome *c* to the peroxidase is complex in the absence of Ca^{2+} (Figure 3a). We propose that this complexity is a reflection of the horse cytochrome *c* binding to the peroxidase monomer and promoting a dimerization which is expressed as a cooperativity. In the presence of Ca^{2+} the titration simplifies (Figure 3b). The stabilization of the enzyme by Ca^{2+} is also evident in differential scanning calorimetry where the unfolding temperature is raised from 43.5 to 52.1 °C. In principle, this may simply be due to the stabilization by Ca^{2+} binding to a single polypeptide chain. However, the elevation of the unfolding temperature is also consistent with a stabilization by Ca^{2+} due to the promotion of the dimeric state. A smaller elevation in the unfolding temperature is seen in the presence of 50 mM NaCl.

The degree of elevation of the unfolding temperature is a function of the affinity of the ligand for the native state and the concentration of ligand (*21*)

$$\ln(1 + [L]/K_d) = \Delta T_m \Delta H°/nRT_{m(L)}T_{m(NL)}$$

where [L] is ligand concentration, K_d is the dissociation constant of the ligand from the native state, ΔT_m is the shift in transition temperature of the protein brought about by the binding, $\Delta H°$ is the enthalpy of the transition, $T_{m(L)}$ is the protein transition temperature in the presence of ligand, $T_{m(NL)}$ is the protein transition temperature in the absence of ligand, and n is the number of sites.

At pH 7.5, in the case of 50 mM NaCl, the ΔT_m of 3.9 °C corresponds to a K_d of approximately 10 mM, while the ΔT_m of 9.4 °C in the case of 2 mM $CaCl_2$ corresponds to a submillimolar K_d, consistent with that observed for Ca^{2+} binding to the enzyme (0.52 mM) in ref *10*.

At pH 6 the thermogram shows the presence of both the 43° and 52° transitions in the absence of added Ca^{2+} (Figure

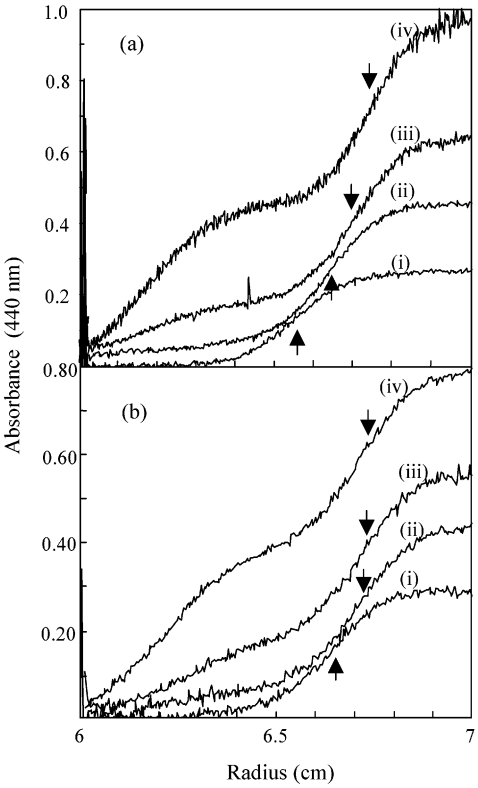

FIGURE 4: Sedimentation velocity boundaries of *Paracoccus* cytochrome *c* peroxidase in the presence of horse cytochrome *c* and cytochrome *c*-550. (a) Binding of horse cytochrome *c* and *Paracoccus* cytochrome *c* peroxidase. Solutions of cytochrome *c* peroxidase (10 μM) in the presence of (i) no horse cytochrome *c*, (ii) 10 μM horse ferricytochrome *c*, (iii) 20 μM horse ferricytochrome *c*, and (iv) 40 μM horse cytochrome *c* were centrifuged at 45000 rpm in 10 mM Mes, 10 mM NaCl, and 2 mM $CaCl_2$, pH 6 at 25 °C. Absorbance scans of the centrifuge cells were done at 440 nm. The scans shown here are taken at equivalent time points for the four experiments. The arrows indicate the midpoints of the leading boundary. (b) Binding of cytochrome *c*-550 and *Paracoccus* cytochrome *c* peroxidase. Solutions of cytochrome *c* peroxidase (10 μM) in the presence of (i) no cytochrome *c*-550, (ii) 10 μM cytochrome *c*-550, (iii) 20 μM cytochrome *c*-550, and (iv) 40 μM cytochrome *c*-550 were centrifuged at 45000 rpm in 10 mM Mes, 10 mM NaCl, and 2 mM $CaCl_2$, pH 6 at 25 °C. Absorbance scans of the centrifuge cells were done at 440 nm. The scans shown here are taken at equivalent time points for the four experiments. The arrows indicate the midpoints of the leading boundary.

3a). This is the pH at which other methods have shown the presence of both monomer and dimer.

We can conclude that Ca^{2+} promotes the dimeric state. The presence of Ca^{2+} therefore leads to an important simplification of solution states, which is necessary if the results of binding with redox partners are to be interpretable. Subsequent binding studies with redox partners were therefore conducted in the presence of Ca^{2+}. We chose to do these experiments at pH 6.0 in the presence of 2 mM Ca^{2+} in order to be confident that dimerization of the peroxidase is essentially complete (which would not be the case at pH 7.5). Under these conditions, the sedimentation equilibrium results are consistent with a fully dimeric protein.

Molar Ratio for Binding of Peroxidase to Horse Cytochrome c and Cytochrome c-550. The leading boundary at high cytochrome *c*-550:cytochrome *c* peroxidase ratios has a *s*/*D* consistent with a molecular weight of 94000. Since the binding of two cytochromes *c*-550 (M_r 14815) to a

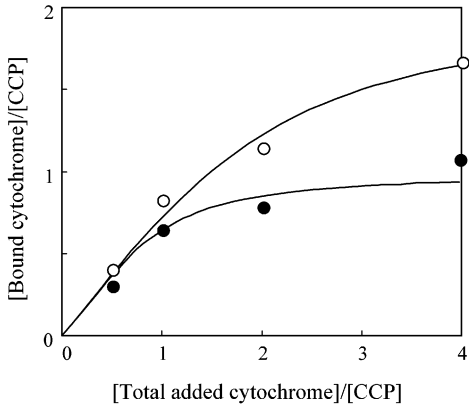

FIGURE 5: Binding of cytochromes to *Paracoccus* cytochrome *c* peroxidase based on analysis of sedimentation velocity profiles: open circles, binding of horse cytochrome *c*; closed circles, binding of *Paracoccus* cytochrome *c*-550. For a given total added cytochrome *c*, the proportion bound to the cytochrome *c* peroxidase could be calculated from the increment in the absorbance of the leading boundary over that due to the peroxidase itself. The proportion of free cytochrome could be calculated from the absorbance at the trailing boundary. When the leading and trailing boundaries were difficult to resolve, the absorbance of the trailing boundary was obtained from a later scan in which the leading boundary had already sedimented. The absorbance values of boundaries were corrected for the radial dilution effect of the sectored cell. The lines are theoretical lines for two sites with a K_d of 5 μM (horse cytochrome *c*) and one site with a K_d of 2 μM for *Paracoccus* cytochrome *c*-550. (For the former, a fit of two independent sites with different K_d values is also possible, but the data were not sufficient to justify this more complex fitting.)

peroxidase dimer (M_r 75026) should yield a particle of M_r 104656, the sedimentation result is consistent with a molar binding ratio of 1:1 but with incomplete occupancy. Such a molar binding ratio is also suggested by the analysis of relative absorbance contributions to the sedimentation boundaries (Figure 5), and the same ratio is found in the isothermal titration calorimetry. Thus these results corroborate the molar binding ratio of 1:1 observed in ^{1}H NMR titrations (*1*). An accurate value of K_d could not be obtained from the ^{1}H NMR experiments, but it was clear that it was less than 5 μM. This is consistent with the K_d of 3−4 μM obtained by microcalorimetry (Table 2).

The leading boundary at high horse cytochrome *c*:cytochrome *c* peroxidase ratios has an *s*/*D* value that yields M_r 108000. Binding of four horse cytochromes *c* (M_r 12361) to a peroxidase dimer would yield a particle of predicted M_r 124470. The plot of Figure 5 indicates that saturation of the two sites per monomer has not been achieved at the solution proportions of 4:1 cytochrome:peroxidase but curve fitting is consistent with a limiting molar binding ratio of 2:1. Simple single-set-of-sites analysis of the isothermal calorimetric titrations of the binding yields *N* values substantially greater than 1 (for example, the 1.64 at pH 7.5 in Table 2). This is suggestive of more than one binding site per monomer, but two identical binding sites are not structurally possible. Thus a more reasonable analysis is that shown in Figure 3d of two independent sites per monomer with different K_d values. These results corroborate the molar binding ratio of 2:1 observed in ^{1}H NMR titrations (*1*). Again, the value of K_d could not be reliably obtained from the previous ^{1}H NMR work, but it was clearly less than 5 μM. This is consistent with the one-site value of 2.2 μM

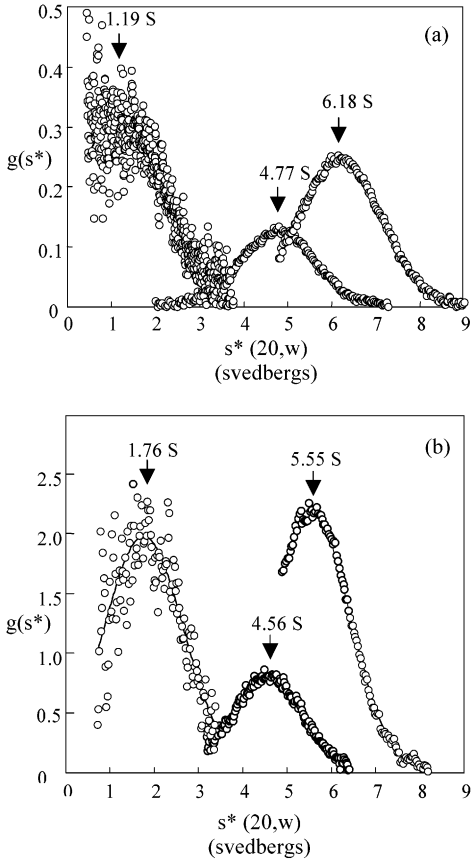

FIGURE 6: Effect of cytochrome *c* binding on the sedimentation coefficient of the *Paracoccus* cytochrome *c* peroxidase. Sedimentation velocity experiments were performed in 10 mM Mes, 10 mM NaCl, and 2 mM $CaCl_2$, pH 6.0, 25 °C, at 45000 rpm. Paired scans within a set of 10 sequential scans were used to produce a distribution of sedimentation coefficients using the DCDT+ method of Philo (*16*) and Stafford (*17*, *18*). For experiments in which two boundaries were evident, both were analyzed. (a) Cytochrome *c* peroxidase (closed circles) and cytochrome *c* peroxidase in the presence of 4 mol/mol horse cytochrome *c* (open circles). (b) Cytochrome *c* peroxidase (closed circles) and cytochrome *c* peroxidase in the presence of 4 mol/mol cytochrome *c*-550 (open circles). In both (a) and (b), the slow boundary represents the free cytochrome *c*. The vertical axis is in absorbance units/Svedberg.

obtained by microcalorimetry under the same conditions (Table 2).

Docking simulations (*1*) indicated that the first horse cytochrome *c* bound preferentially at a between-hemes site which we would now equate with the high-affinity site seen in isothermal calorimetry. It seems likely that the low-affinity binding site for horse cytochrome *c* might be the E site favored by cytochrome *c*-550. As a test of this hypothesis, we have simulated the docking of horse cytochrome *c* to a cytochrome *c* peroxidase molecule with a horse cytochrome *c* molecule already bound to it at the between-hemes site.

To do this, we have used the original BiGGER algorithm that we had used in ref *1*. The original algorithm dealt with the probe and target proteins as rigid bodies and applied stringent geometric filtering to generate the group of 1000 candidate solutions. This algorithm has evolved through several optimizing stages (see http://www.dq.fct.unl.pt/bioin/chemera/) to allow "softer" docking in which surface side chains are truncated. This allows better capture of correct solutions in some model cases but introduces a higher level of "noise" in others. In our particular case the original "hard" docking has always led to efficient capture of complexes which were seen as likely candidates on the basis of other criteria such as Fe−Fe distances and ^{1}H NMR perturbations. Typically, in the top 10 or 20 solutions of the ranked set, a majority formed a cluster at a particular position and orientation of one protein relative to the other (*1*). It may be that the success of the original hard-docking version of BiGGER when applied to these electron transfer proteins is a true reflection of the distinct nature of the complexes where side chains may not form particularly intimate contacts due to the presence of interface water, and global electrostatic effects become the major determinant.

The results shown in Figure 7 indicate that the most favored secondary site for the horse cytochrome *c* in this instance is the E heme site. The top-ranking solution has a global score not too different (−68 vs −72) from the top between-hemes solution that was used as the target (*1*). Since E solutions were rare and poorly ranked in the original dock, this may imply cooperativity and a sequential binding process. The Fe−Fe distance for the horse cytochrome *c* bound at the E position is 17 Å, very similar to the 16 Å obtained for the E complex of cytochrome *c*-550 and the cytochrome *c* peroxidase (*1*) and similar to iron−iron distances observed in other heme/heme electron transfer complexes [most recently the cytochrome *c*/cytochrome bc_1 complex (*22*)].

Thermodynamic Parameters of Binding and the Nature of the Interface. The analysis of the heat changes associated with the binding of the proteins in Mes and cacodylate buffers allows an estimate of the true $\Delta H°$ for binding and the calculation of the number of protons released (and taken up by the buffer) on complex formation. The results in Table 2 indicate that this correction to $\Delta H°$ enhances the already striking pattern of a strongly unfavorable enthalpy change countered by an even more strongly favorable entropy change. We cannot say whether the fractional proton release in each experiment is due to a single ionizable group or the combination of several, nor do we know whether the fractional proton originates on the donor cytochromes or on the peroxidase.

The thermodynamic parameters governing the association of two proteins are the result of a number of complex contributions. The enthalpy change will have contributions from both bond formation (due to formation of electrostatic links, for example) and bond breakage (due to loss of water from these groups). The entropy change will have contributions from the loss of protein mobility and the increased disorder of the water molecules as they are lost from the interface.

The binding of cytochromes to cytochrome *c* peroxidase is endothermic (positive $\Delta H°$) and, consequently, entropy driven (positive $\Delta S°$) under all conditions examined here. This is consistent with the displacement of interfacial water as the major driving force for protein/protein association in this system, as has been suggested for the related (but structurally rather different) yeast cytochrome *c* peroxidase when binding horse cytochrome *c* (Table 2; *23*). However, we should note that the binding of the yeast peroxidase to its own yeast iso-1-cytochrome *c* is characterized by a strongly favorable enthalpy change and a correspondingly much smaller entropy contribution (Table 2; *24*).

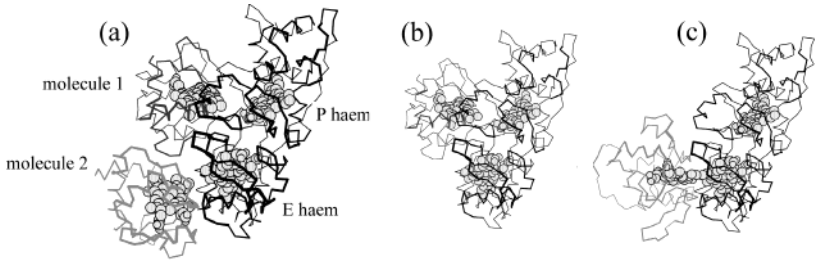

FIGURE 7: Docking simulation for a second molecule of horse cytochrome *c* binding to *Paracoccus* peroxidase. The highest ranking solution obtained from the docking of horse cytochrome *c* to *Paracoccus* cytochrome *c* peroxidase in ref *1* [shown here in (b)] was used as a target for the docking of a second molecule of horse cytochrome *c*. Docking was performed using the algorithm BiGGER developed by Palma et al. (*20*). The highest ranking solution is shown in (a). The global score for this solution (which is a composite of the individual evaluations of electrostatics, surface complementarity, solvation energies, and side chain interactions) was −68 in comparison to the global score for the formation of the target shown in (b) of −72 (more negative is more favored). The top 20 solutions had global scores in the range −55 to −68 and contained 12 solutions docked at the E heme. In the original dock of horse cytochrome *c* to the cytochrome *c* peroxidase, the highest ranking solution at the E position was ranked 12th with a global score of −62. (c) is the highest ranking solution from the docking of *Paracoccus* cytochrome *c*-550 to the *Paracoccus* cytochrome *c* peroxidase and shows the binding of the cytochrome *c*-550 close to the E heme of the cytochrome *c* peroxidase.

What is less clear is whether the displaced waters come from specific electrostatic interactions (salt bridge formation) at the protein/protein interface or from more general solvation effects. Kauzmann (*25*) showed how, in addition to the classic hydrophobic effect and contrary to intuition, attractive electrostatic interactions between oppositely charged groups in water might be expected to be endothermic, because of the release of solvated water molecules, with the thermodynamic driving force arising from the entropy gained by the liberated waters. Consequently, both hydrophobic and electrostatic interactions are likely to have similar thermodynamic signatures, and it is difficult to disentangle the effects of different kinds of interactions from thermodynamic data alone. This conclusion has been supported by work in several other systems (*26*−*30*).

Effect of Ionic Strength on Binding and Kinetics and Nature of the High-Affinity Binding Site for Horse Cytochrome c. The reduction in binding affinity for horse cytochrome *c* (3-fold) that we see here with doubling of the ionic strength (Table 2) is associated with a sizable reduction in $\Delta S°$, partly countered by a small fall in $\Delta H°$. The same sizable reduction in $\Delta S°$ is observed for the horse cytochrome *c* binding to the yeast cytochrome *c* peroxidase (Table 2). These results may be due to a general ion screening effect, reflecting changes in the thermodynamics of transfer of interfacial water molecules to the bulk solvent. They might also be a consequence of less rigid complex formation at higher ionic strength, allowing retention of more waters at the protein/protein interface. It is interesting that such a rise in ionic strength has very little effect on the binding of cytochrome *c*-550 to the peroxidase (Table 2), and it is revealing to relate these results to the ionic strength dependence of steady-state kinetics. In the case of horse cytochrome *c* binding to both the yeast (*31*) and the *Paracoccus* (*13*) enzymes, increasing ionic strength in this region of low ionic strength is associated with an increase in enzymic activity (and this then falls away at higher ionic strengths in a fashion predicted for electrostatic complexes). In contrast, the kinetics of oxidation of cytochrome *c*-550 by the *Paracoccus* enzyme is independent of ionic strength in this range (*13*).

A related finding with the yeast peroxidase (*6*) is that intramolecular electron transfer rates within the complex with horse cytochrome *c* are increased by raising the ionic strength between 0.008 and 0.03 M.

One interpretation of this is that, at very low ionic strength, the complex with horse cytochrome *c* is locked in a relatively unproductive orientation by strong specific electrostatic bonds and that raising the ionic strength loosens the association and allows lateral search for a productive orientation. According to this model, the cytochrome *c*-550 may be able to find the correct orientation for electron transfer even at low ionic strength. This interpretation has implications for whether the distinct between-hemes binding site observed for horse cytochrome *c* in molecular docking simulation and ^{1}H NMR spectroscopy (*1*) is actually an electron transfer site. A model in which the peroxidase contains two sites for binding two electron donor proteins simultaneously has some attraction since it allows a coordinated reduction of the oxidized enzyme produced by hydrogen peroxide and containing two oxidizing equivalents. However, our present results indicate that horse cytochrome *c*, captured on the side of the peroxidase, may become trapped at low ionic strength in a nonproductive orientation. We propose that this is the higher affinity between-hemes binding detected by ^{1}H NMR spectroscopy and molecular docking and, in this paper, by isothermal microcalorimetry. We propose that the lower affinity site detected by isothermal microcalorimetry is the actual electron transfer site at the E heme. One could regard the high-affinity nonproductive binding of horse cytochrome *c* as an artifact resulting from the use of a nonphysiological electron donor which has not evolved to optimize its interaction with the peroxidase. However, it is quite a useful artifact because it has allowed detection of the process of capture at a broad electrostatic surface followed by a process of lateral translation. In the case of the physiological cytochrome *c*-550, that lateral translation proceeds to the energy minimum of the electron transfer site without trapping en route even at low ionic strength.

An interface populated by water molecules and stabilized by global electrostatic effects rather than specific electrostatic linkages may be a common feature of electron transfer complexes. These relatively low affinity complexes will facilitate mobility and the capacity to search during an encounter and then permit dissociation of the enzyme/product

complex. The retention of key water molecules may also be required to mediate the electron transfer process (*32*, *33*).

ACKNOWLEDGMENT

We thank Ludwig Krippahl in the laboratory of Professors Isabel and Jose Moura for many helpful discussions on the use of the docking algorithm BiGGER and Sofia Pauleta for helpful comments on the manuscript.

REFERENCES

1. Pettigrew, G. W., Prazeres, S., Costa, C., Palma, N., Krippahl, L., and Moura, J. J. (1999) The structure of an electron transfer complex containing a cytochrome *c* and a peroxidase, *J. Biol. Chem. 274*, 11383−11389.
2. Page, C. C., Moser, C. C., Chen, X., and Dutton, P. L. (1999) Natural engineering principles of electron tunnelling in biological oxidation−reduction, *Nature 402*, 47−52.
3. Koppenol, W. H., Rush, J. D., Mills, J. D., and Margoliash, E. (1991) The dipole moment of cytochrome *c*, *Mol. Biol. Evol. 8*, 545−558.
4. Northrup, S. H., Boles, J. O., and Reynolds, J. C. L. (1988) Brownian dynamics of cytochrome *c* and cytochrome *c* peroxidase association, *Science 241*, 67−70.
5. Castro, G., Boswell, C. A., and Northrup, S. H. (1998) Dynamics of protein−protein docking: cytochrome *c* and cytochrome *c* peroxidase revisited, *J. Biomol. Struct. Dyn. 16*, 413−424.
6. Hazzard, J. T., Moench, S. J., Erman, J. E., Satterlee, J. D., and Tollin, G. (1988) Kinetics of intracomplex electron transfer and of reduction of the components of covalent and noncovalent complexes of cytochrome *c* and cytochrome *c* peroxidase by free flavin semiquinones, *Biochemistry 27*, 2002−2008.
7. Liang, Z. X., Nocek, J. M., Huang, K., Hayes, R. T., Kimikov, I. V., Beratan, D. N., and Hoffman, B. M. (2002) Dynamic docking and electron transfer between Zn-myoglobin and cytochrome b_5, *J. Am. Chem. Soc. 124*, 6849−6859.
8. Pelletier, H., and Kraut, J. (1992) Crystal structure of a complex between electron transfer partners, cytochrome *c* peroxidase and cytochrome *c*, *Science 258*, 1748−1755.
9. Leesch, V. W., Bujous, J., Mauk, A. G., and Hoffman, B. M. (2000) Cytochrome *c* peroxidase-cytochrome *c* complex: locating the second binding domain on cytochrome *c* peroxidase with site-directed mutagenesis, *Biochemsitry 39*, 10132−10139.
10. Gilmour, R., Prazeres, S., McGinnity, D. F., Goodhew, C. F., Moura, J. J. G., Moura, I., and Pettigrew, G. W. (1995) The binding of Ca^{++} to cytochrome *c* peroxidase from *Paracoccus denitrificans*—affinity and specificity of sites, *Eur. J. Biochem. 234*, 878−886.
11. Hu, W., Van Driesche, G., Devreese, B., Goodhew, C. F., McGinnity, D. F., Saunders, N., Fulop, V., Pettigrew, G. W., and van Beeumen, J. J. (1997) Structural characterisation of *Paracoccus denitrificans* cytochrome *c* peroxidase and assignment of the low and high potential heme sites, *Biochemistry 36*, 7958−7966.
12. Gilmour, R., Goodhew, C. F., Pettigrew, G. W., Prazeres, S., Moura, I., and Moura, J. J. (1993) Spectroscopic characterization of cytochrome *c* peroxidase from *Paracoccus denitrificans*, *Biochem. J. 294*, 745−752.
13. Gilmour, R., Goodhew, C. F., Pettigrew, G. W., Prazeres, S., Moura, J. J., and Moura, I. (1994) The kinetics of the oxidation of cytochrome *c* by Paracoccus cytochrome *c* peroxidase, *Biochem. J. 300*, 907−914.
14. Rainey, F. A. (1994) A reevaluation of the taxonomy of *Paracoccus denitrificans* and a proposal for the creation of *Paracoccus pantotrophus* comb.nov, *Int. J. Syst. Bacteriol. 49*, 645−651.
15. Goodhew, C. F., Wilson, I. B., Hunter, D. J., and Pettigrew, G. W. (1990) The cellular location and specificity of bacterial cytochrome *c* peroxidases, *Biochem. J. 271*, 707−712.
16. Philo, J. S. (2001) A method for directly fitting the time derivative of sedimentation velocity data and an alternative algorithm for calculating sedimentation coefficient distribution functions, *Anal. Biochem. 279*, 151−163.
17. Stafford, W. F. (1994) Boundary analysis in sedimentation velocity experiments, *Methods Enzymol. 240*, 478−501.
18. Stafford, W. F. (1992) Boundary analysis in sedimentation transport experiments: A procedure for obtaining sedimentation coefficient distributions using the time derivative of the concentration profile, *Anal. Biochem. 203*, 295−301.
19. Laue, T. M., Shah, B. D., Ridheway, T. M., and Pelletier, S. L. (1992) Computer-aided interpretation of sedimentation data for proteins, in *Analytical Ultracentrifugation in Biochemistry and Polymer Science* (Harding, S. E., Rowe, A. J., and Horton, J. C., Eds.) pp 90−125, Royal Society of Chemistry, London.
20. Palma, P. N., Krippahl, L., Wampler, J. E., and Moura, J. J. G. (2000) BiGGER—a new (soft) docking algorithm for predicting protein interactions, *Proteins 39*, 372−384.
21. Cooper, A., and McAuley-Hecht, K. E. (1993) Microcalorimetry and the molecular recognition of peptides and proteins, *Philos. Trans. R. Soc. London, Ser. A 345*, 23−35.
22. Lange, C., and Hunte, C. (2002) Crystal structure of the yeast cytochrome bc_1 complex bound cytochrome *c*, *Proc. Natl. Acad. Sci. U.S.A. 99*, 2800−2805.
23. Kresheck, G. C., Vitello, L. B., and Erman, J. E. (1995) Calorimetric studies on the interaction of horse ferricytochrome *c* and yeast cytochrome *c* peroxidase, *Biochemistry 34*, 8398−8405.
24. Wang, X., and Pielak, G. J. (1999) Equilibrium thermodynamics of a physiologically-relevant heme-protein complex, *Biochemistry 38*, 16876−16881.
25. Kauzmann, W. (1959) Some factors in the interpretation of protein denaturation, *Adv. Protein Chem. 14*, 1−63.
26. Ortiz-Salmeron, E. M., Baron, C., and Garcia-Fuentes, L. (1998) Enthalpy of captopril-angiotensin I-converting enzyme binding, *FEBS Lett. 435*, 219−224.
27. Velasquez-Campoy, A., Todd, M. J., and Freire, E. (2000) The binding energetics of first and second generation HIV-1 Protease inhibitors: implications for drug design, *Biochemistry 39*, 2201−2207.
28. Cooper, A. (1999) Thermodynamic analysis of biomolecular interactions, *Curr. Opin. Chem. Biol. 3*, 557−563.
29. Cooper, A., Johnson, C. M., Lakey, J. H., and Nollman, M. (2001) Heat does not come in different colours: entropy-enthalpy compensation, free energy windows, quantum confinement, pressure perturbation calorimetry, solvation and the multiple causes of heat capacity effects in biomolecular interactions, *Biophys. Chem. 93*, 215−230.
30. Jung, H., Bowden, S. J., Cooper, A., and Perham, R. N. (2002) Thermodynamic analysis of the binding of component enzymes in the assembly of the pyruvate dehydrogenase multienzyme complex of *Bacillus stearothermophilus*, *Protein Sci. 11*, 1091−1100.
31. Kang, C. H., Ferguson-Miller, S., and Margoliash, E. (1977) Steady-state kinetics and binding of eukaryotic cytochrome *c* with yeast cytochrome *c* peroxidase, *J. Biol. Chem. 252*, 919−926.
32. Ferguson-Miller, S. (2001) Substrate docking and electron transfer in cytochrome *c* oxidase, *J. Inorg. Biochem. 86*, 47.
33. Tezcan, F. A., Crane, B. R., Winkler, J. R., and Gray, H. B. (2001) Electron tunneling in protein crystals, *Proc. Natl. Acad. Sci. U.S.A. 98*, 5002−5006.

BI027125W